University of Groningen

Bachelor Project Applied Mathematics

The effect of vegetation on water flow

First supervisor:
Dr. Julian Koellermeier

Author:
Jesse Bruinsma *(s4053125)*

Second supervisor:
Dr. Fred Wubs

Daily supervisor:
Rik Verbiest

Abstract

Shallow water moment equations are a set of partial differential equations which can describe the water flow accurately by allowing different horizontal velocities over the vertical scale. These equations where derived from the incompressible Navier-Stokes equation. What these models do not take into account is aquatic vegetation in rivers. Vegetation can appear in various types and shapes and each interact with the water flow differently. In this paper the important ideas for deriving the shallow moment system will be reviewed. Using these ideas the shallow water moment system with rigid submerged and emergent vegetation will be derived by including a friction term for the vegetation in the momentum balance equation. In this new model the friction increase over the vegetation height gives logical and explainable observations.

June 26, 2024

1 Introduction

The Shallow Water Equations (SWE) are a set of partial differential equations which are used to model the flow in scenarios where the horizontal scales are much greater than the vertical scales. Such scenarios can be oceans, rivers, coastal areas and lakes. The SWE can be implemented in a wide range of applications in different scientific fields. They are for example used in modelling tsunamis [12] or weather forecasting [22]. An important note to make is that SWE are limited in their applications since it averages the vertical velocity. Averaging the vertical velocity is a strong simplification and it has been shown that it renders inaccurate numerical simulations. In many situations, the velocity of the water flow is lower on the bottom, than in another water layer in the river due to friction. Furthermore, due to strong winds blowing over the water surface, a higher flow velocity will be generally measured in the top layer than at any other depth.

To solve these problems, the Shallow Water Moments Equations (SWME) were derived [14]. These equations allow for different horizontal velocities that depend on the vertical coordinate. The SWME system is obtained by using the method of moments, which includes the expansion of the vertical flow velocity in a polynomial basis and a subsequent Galerkin projection to obtain evolution equations for the expansion coefficients [14]. These equations render a more accurate approximation in describing the water flow than the SWE. A disadvantage of the SWME is that it is not globally hyperbolic. The lack of hyperbolicity can lead to unstable numerical simulations. To resolve this lack of hyperbolicity a hyperbolic regularization is derived by modifying the system matrix resulting in the hyperbolic shallow water moment equations [13].

Another variable which the SWME system does not take into account is aquatic vegetation in rivers. Aquatic vegetation occurs in most rivers and other types of waters. Vegetation can appear in numerous variations, from sea grasses and algae to mangroves and reefs, each interacting differently with the flow. Vegetation can be rigid or flexible and it can even be further classified into submerged, emergent or floating vegetation. The presence of vegetation stimulates slowing down river erosion and stabilizing floodplains or riverbanks [2]. Furthermore, they also absorb pollutants and promote oxidation which improves the self-purification ability of the river [9]. Vegetation also provides for a suitable habitat for aquatic animals which contributes to the development of the diversity in aquatic species [17].

The importance of doing research into the SWE with vegetation is high, since at this moment there is still no theory which accommodates all the classification of different types of vegetation [9]. It can also help in all sorts of practical implications in environmental engineering and management. For instance in Coastal engineering, modeling how mangroves and other coastal plants attenuate wave energy is crucial for developing nature-based solutions to coastal protection [7, 21].

The aim of this paper is to investigate SWME and modify these equations by including a vegetation friction term. By including this term we can find a set of equations which can describe the flow in rivers with vegetation. Because of the complex geometry of real plants, the aquatic vegetation is often simplified to rigid circular cylinder array with uniform diameter, which is a reasonable generalization for plants with fewer branches and leaves below the water surface [9]. This simplified representation of the aquatic vegetation will also be used in this paper.

Before we derive the new set of equations for a river flow with vegetation, we will start at the beginning and lay the focus on how the SWME system is derived using [14]. Using this information we are going to research how other papers investigated the river flow with vegetation. The information gained here will be used to find the new SWME with vegetation. Here we are going to investigate how these equations will look like for rigid emergent and submerged

vegetation.

The structure of the paper is as follows: In section 2 an explanation will be given on how the SWME are derived with the help of two important ideas. An short overview will be given in section 3 on research which has been done in modelling the shallow water flow. In section 4 the information obtained in section 2 and 3 will be used to derive the SWME system for rigid vegetation. This will first be done for emergent vegetation in 4.1 and then for submerged in 4.2. In section 5 an analysis will be given for the SWME system with rigid vegetation.

2 The Shallow Water Moments Equations

In this section the two main ideas will be shown on how the shallow water moment system is derived. It is important to have these ideas clear before we can include the effect of vegetation on the flow. We refer to [14] for any major calculations.

The starting point of deriving the SWME are the incompressible Navier-Stokes equations. These equations can be reduced by an asymptotic analysis implied by the shallowness assumption $\left(\frac{H}{L} \ll 1\right)$ [14], H is the fluid depth and L is the horizontal scale of motion, resulting in the following mass and momentum balance equations

$$\frac{\partial u}{\partial x} + \frac{\partial v}{\partial y} + \frac{\partial w}{\partial z} = 0, \tag{1}$$

$$\frac{\partial u}{\partial t} + \frac{\partial u^2}{\partial x} + \frac{\partial uv}{\partial y} + \frac{\partial uw}{\partial z} = -\frac{1}{\rho}\frac{\partial p}{\partial x} + \frac{1}{\rho}\frac{\partial \sigma_{xz}}{\partial z} + ge_x, \tag{2}$$

$$\frac{\partial v}{\partial t} + \frac{\partial vu}{\partial x} + \frac{\partial v^2}{\partial y} + \frac{\partial vw}{\partial z} = -\frac{1}{\rho}\frac{\partial p}{\partial y} + \frac{1}{\rho}\frac{\partial \sigma_{yz}}{\partial z} + ge_y. \tag{3}$$

Here we have that the state variables $\mathbf{u}= (u, v, w)^T$ are the velocities, p denotes the pressure and σ is the deviatoric stress tensor. All these variables depend on space (x, y, z) and time t. Where the hydrostatic pressure is given by

$$p(x, y, z, t) = (h_s(x, y, t) - z)\, \rho g e_z, \tag{4}$$

where $h_s(x, y, t)$ indicates the water surface height. Furthermore ρ is the density which is constant and g indicates the gravitational acceleration. Finally we have that $(e_x, e_y, e_z)^T$ is a unit vector.

The first important step in deriving the SWME is to transform our reference system with respect to the z direction into a scaled space where we introduce the following scaled vertical variable $\zeta(x, y, t)$ using

$$\zeta(x, y, t) = \frac{z - h_b(x, y, t)}{h(x, y, t)}. \tag{5}$$

Here the water height is defined as $h(x, y, t) = h_s(x, y, t) - h_b(x, y, t)$ from the bottom h_b to the water surface h_s, hence we have that $\zeta \in [0, 1]$. This mapping implies that $z = \zeta h(x, y, t) + h_b(x, y, t)$ (see figure 1). Using these mappings we can transform the governing equation (see figure. Given an arbitrary function which depends on space and time S, then we can compute its mapped counterpart by

$$\hat{S}(x, y, \zeta, t) = S(x, y, \zeta h(x, y, t) + h_b(x, y, t), t), \tag{6}$$

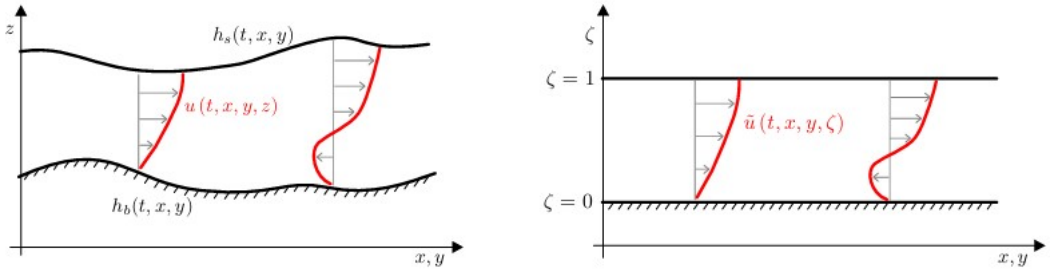

Figure 1: In the physical space (left) the flow is constrained in the z-direction between the bottom topography h_b and the water surface h_s. Using the mapping (5) the flow is constrained in the projected depth coordinate ζ-direction between 0 and 1 (right) [14].

Which implies

$$S(x,y,z,t) = \hat{S}\left(x,y,(z-h_b(x,y,t))\,h(x,y,t)^{-1},t\right). \tag{7}$$

The method to transform the differential operators of the mappings works as follows

$$h\frac{\partial S}{\partial n} = \frac{\partial h\hat{S}}{\partial n} - \frac{\partial}{\partial \zeta}\left(\frac{\partial}{\partial n}\left(\zeta h + h_b\right)\hat{S}\right), \text{ for } n \in \{x,y,t\}, \tag{8}$$

$$h\frac{\partial S}{\partial z} = \frac{\partial \hat{S}}{\partial \zeta}. \tag{9}$$

Multiplying h with the mass and momentum balance equations (1)-(3) and using the transformation rules mentioned above (6)-(9), the complete vertically resolved shallow flow model according to [14] has the following form

$$\frac{\partial h}{\partial t} + \frac{\partial}{\partial x}\left(hu_m\right) + \frac{\partial}{\partial y}\left(hv_m\right) = 0, \tag{10}$$

$$\frac{\partial}{\partial t}\left(h\hat{u}\right) + \frac{\partial}{\partial x}\left(h\hat{u}^2 + \frac{g}{2}e_z h^2\right) + \frac{\partial}{\partial y}\left(h\hat{u}\hat{v}\right) + \frac{\partial}{\partial \zeta}\left(h\hat{u}\omega - \frac{1}{\rho}\hat{\sigma}_{xz}\right) = gh\left(e_x - e_z\frac{\partial h_b}{\partial x}\right), \tag{11}$$

$$\frac{\partial}{\partial t}\left(h\hat{v}\right) + \frac{\partial}{\partial x}\left(h\hat{v}\hat{u}\right) + \frac{\partial}{\partial y}\left(h\hat{v}^2 + \frac{g}{2}e_z h^2\right) + \frac{\partial}{\partial \zeta}\left(h\hat{v}\omega - \frac{1}{\rho}\hat{\sigma}_{yz}\right) = gh\left(e_y - e_z\frac{\partial h_b}{\partial y}\right). \tag{12}$$

Where $u_m = \int_0^1 \hat{u}d\zeta$ and $v_m = \int_0^1 \hat{v}d\zeta$ denotes the mean velocity in the respective x and y direction. The vertical coupling operator ω is defined by

$$h\omega = -\frac{\partial}{\partial x}\left(h\int_0^\zeta \hat{u} - u_m d\tilde{\zeta}\right) - \frac{\partial}{\partial y}\left(h\int_0^\zeta \hat{v} - v_m d\tilde{\zeta}\right). \tag{13}$$

observing the balance equations (10)-(12) it can be seen that these equations have a lot in common with the SWE. This is definitely true for the mass balance equation (10). In case of the momentum balance equations, for a constant flow in ζ the vertical coupling term ω will vanish. If the shear stresses will be negligible meaning that $\hat{\sigma}_{xz} = \hat{\sigma}_{yz} = 0$, the whole system (10)-(12) reduces to the frictionless shallow water equations.

The next step is to examine the momentum balance equation (11) and use the Newtonian relations from [14]. For readability we drop the hat and calculate the integral with respect to ζ from 0 to 1

$$\int_0^1 \left(\frac{\partial}{\partial t}(hu) + \frac{\partial}{\partial x}\left(hu^2 + \frac{g}{2}e_z h^2\right) + \frac{\partial}{\partial y}(huv) + \frac{\partial}{\partial \zeta}\left(hu\omega - \frac{\nu}{h}\frac{\partial u}{\partial \zeta}\right)\right) d\zeta = \int_0^1 \left(gh(e_x - e_z \frac{\partial h_b}{\partial x})\right) d\zeta,$$

$$\Rightarrow \frac{\partial}{\partial t}(hu_m) + \frac{\partial}{\partial x}\left(h\int_0^1 u^2 d\zeta + \frac{g}{2}e_z h^2\right) + \frac{\partial}{\partial y}\left(h\int_0^1 uv d\zeta\right) + \left[\frac{\nu}{\lambda}u\right]_{\zeta=0} = gh\left(e_x - e_z\frac{\partial h_b}{\partial x}\right). \tag{14}$$

This is called the evolution equation for the mean velocity u_m. We used the fact that the vertical coupling operator ω vanishes at the top and bottom. The constants ν and λ are respectively the kinematic viscosity and the slip length.

The second main step in deriving the shallow water moment system, is writing both lateral velocity components u and v as the sum of the mean velocities and its deviation which is modelled by a finite polynomial expansion also known as the moment expansion [14]

$$u(x,y,\zeta,t) = u_m(x,y,t) + \sum_{j=1}^{N} \alpha_j(x,y,t)\,\phi_j(\zeta), \tag{15}$$

$$v(x,y,\zeta,t) = v_m(x,y,t) + \sum_{j=1}^{N} \beta_j(x,y,t)\,\phi_j(\zeta). \tag{16}$$

Where ϕ_j denotes the shifted and scaled Legendre polynomials of degree j. The variables α_j and β_j are the corresponding basis coefficients, also known as the moments for respective velocities u and v. These moments will give rise to different horizontal velocities over the height. This is an extension compared to the classical SWE where the horizontal velocity does not change over the height. The scaled Legendre polynomials ϕ_j have the property that they are orthogonal in the interval $[0,1]$. Lastly, $N \in \mathbb{N}$ denotes the degree of the largest polynomial to which we describe the velocity profile. Increasing this coefficient will render in a better approximation of the velocity profile.

Using the expansions of (15)(16) and the properties of the scaled Legendre polynomials, we can write out the integrals from equation (14) as follows

$$\int_0^1 u^2 d\zeta = u_m^2 + \sum_{j=1}^{N} \frac{\alpha_j^2}{2j+1}, \quad \int_0^1 uv\,d\zeta = u_m v_m + \sum_{j=1}^{N} \frac{\alpha_j \beta_j}{2j+1}. \tag{17}$$

Inserting this in (14), we obtain the equation

$$\frac{\partial}{\partial t}(hu_m) + \frac{\partial}{\partial x}\left(h\left(u_m^2 + \sum_{j=1}^{N}\frac{\alpha_j^2}{2j+1}\right) + \frac{g}{2}e_z h^2\right) + \frac{\partial}{\partial y}\left(h\left(u_m v_m + \sum_{j=1}^{N}\frac{\alpha_j\beta_j}{2j+1}\right)\right) = -\frac{\nu}{\lambda}\left(u_m + \sum_{j=1}^{N}\alpha_j\right) + gh\left(e_x - e_z\frac{\partial h_b}{\partial x}\right). \tag{18}$$

Analogously the same yields for the averaging the y-momentum balance

$$\frac{\partial}{\partial t}\left(hv_m\right)+\frac{\partial}{\partial y}\left(h\left(v_m^2+\sum_{j=1}^{N}\frac{\beta_j^2}{2j+1}\right)+\frac{g}{2}e_z h^2\right)+\frac{\partial}{\partial x}\left(h\left(v_m u_m+\sum_{j=1}^{N}\frac{\alpha_j\beta_j}{2j+1}\right)\right)= -\frac{\nu}{\lambda}\left(v_m+\sum_{j=1}^{N}\beta_j\right)+gh\left(e_y-e_z\frac{\partial h_b}{\partial y}\right). \quad (19)$$

When the deviations from the mean can be neglected all the coefficients α_j and β_j will be zero and we will return back to the SWE.

If this is not the case we need equations for the moments coefficients α_i and β_i. We do this by multiplying the scaled Legendre polynomial ϕ_i of degree i with the expansions (15)(16) resulting in

$$\int_0^1 \phi_i u d\zeta=\frac{\alpha_i}{2i+1},\quad \int_0^1 \phi_i v d\zeta=\frac{\beta_i}{2i+1}. \quad (20)$$

These equations are used to obtain the evolution equation for α_i and β_j which look like

$$\frac{\partial}{\partial t}\left(h\alpha_i\right)+\frac{\partial}{\partial x}\left(h\left(2u_m\alpha_i+\sum_{j,k=1}^{N}\alpha_j\alpha_k A_{ijk}\right)\right)+\frac{\partial}{\partial y}\left(h\left(u_m\beta_i+v_m\alpha_i+\sum_{j,k=1}^{N}\alpha_j\beta_k A_{ijk}\right)\right)= u_m D_i-\sum_{j,k=1}^{N}\alpha_k B_{ijk}D_i-(2i+1)\frac{\nu}{\lambda}\left(u_m+\sum_{j=1}^{N}\left(1+\frac{\lambda}{h}C_{ij}\right)\alpha_j\right), \quad (21)$$

$$\frac{\partial}{\partial t}\left(h\beta_i\right)+\frac{\partial}{\partial y}\left(h\left(2v_m\beta_i+\sum_{j,k=1}^{N}\beta_j\beta_k A_{ijk}\right)\right)+\frac{\partial}{\partial x}\left(h\left(v_m\alpha_i+u_m\beta_i+\sum_{j,k=1}^{N}\alpha_j\beta_k A_{ijk}\right)\right)= v_m D_i-\sum_{j,k=1}^{N}\beta_k B_{ijk}D_i-(2i+1)\frac{\nu}{\lambda}\left(v_m+\sum_{j=1}^{N}\left(1+\frac{\lambda}{h}C_{ij}\right)\beta_j\right). \quad (22)$$

Where we have that

$$A_{ijk}=(2i+1)\int_0^1\phi_i\phi_j\phi_k d\zeta,\ B_{ijk}=(2i+1)\int_0^1\phi_i'\left(\int_0^\zeta\phi_j d\hat{\zeta}\right)\phi_k d\zeta, \quad (23)$$

$$C_{ij}=\int_0^1\phi_i'\phi_j' d\zeta \text{ and } D_i=\frac{\partial}{\partial x}\left(h\alpha_i\right)+\frac{\partial}{\partial y}\left(h\beta_i\right). \quad (24)$$

The details of the derivation of the evolution equations and the matrices A_{ijk}, B_{ijk} and C_{ij} are given in [14]. An important thing to note here is that N indicates the order of the moment system and i denotes the actual equation for the specific moment α_i and β_i.

One problem of the SWME is that it is not globally hyperbolic. Hyperbolicity generally implies well-posedness and stability for quasi-linear, first order partial differential equations and is an important property for not only modelling flow problems in hydrodynamics, but also in modelling the flow in other fields like gas dynamics [4, 15]. The lack in hyperbolicity can lead to uncontrolled growth of linear instabilities and unwanted grid dependencies.

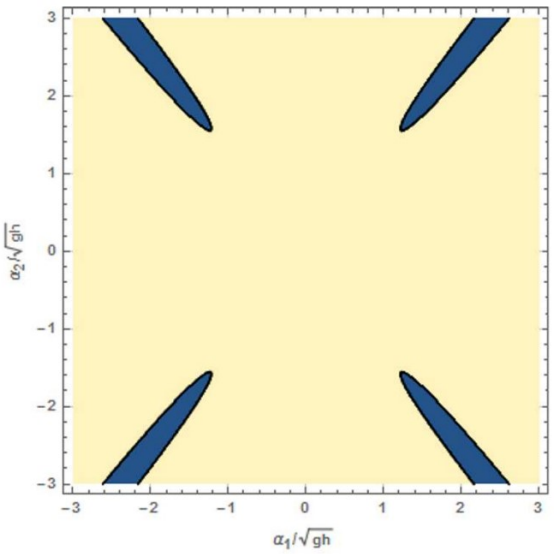

Figure 2: The hyperbolic regions of the quadratic system $N = 2$. The beige area denotes the hyperbolic region where the eigenvalues are real. The blue area denotes the occurrence of complex eigenvalues and hence have a hyperbolic breakdown [13].

In context with the shallow water moment system, a lack in hyperbolicity can lead to a presence of complex eigenvalues in certain regions of the state space. Figure 2 gives a visualization for the quadratic case $N = 2$. Where we have a lack in hyperbolicity in the blue region and the beige area is the hyperbolic region. The break down of hyperbolicity in the shallow moment system can be associated with a degeneracy of the associated vertical velocity profiles or inappropriate projection of these profiles.

To deal with the loss of hyperbolicity, [13] uses two approaches. In the first approach, all coefficients α_i of the system matrix are set to zero, except for α_1. The resulting system is called the Hyperbolic Shallow Water Moments Equations (HSWME) using a modified system matrix A_H. In the second approach a generalization of the first approach is used, where hyperbolicity is guaranteed by introducing a new parameter β_i to the last row of the system matrix A_H. The new system matrix is denoted by A_β and the system is called the generalized β-Hyperbolic Shallow Water Moment Equations (β-HSWME).

Other ways to deal with the lack of hyperbolicity can be by using different projection techniques based on quadrature for example [6]. An alternative approach was proposed in the field of kinetic gas theory which relies on a non-linear maximum entropy approach [16]. The rest of the paper will not consider hyperbolicity of the system, since we only want to investigate what the effect of vegetation is on the water flow.

3 Study of vegetation

In this section, a short review will be given about research which has been done in modelling shallow water flow with vegetation.

Vegetation can appear in numerous ways and can have a very complex geometry. To analyse how these kinds of vegetation with complex geometry will interact with the water flow is com-

plicated. A solution to this problem is to simplify the representation of the vegetation into an array without branches [20]. Here they mimic the behaviour of sea grasses by using sea grass surrogates. How these surrogates interacts with the water flow depends highly on the chosen mechanic and properties of the surrogates. To measure the instantaneous velocity fields in the vicinity and wake of the surrogates a stereoscopic particle image velocimetry is used, where all employed surrogates disrupt and interact with the flow by changing their posture.

Since flexible vegetation can still be hard to model mathematically, aquatic vegetation is usually represented as rigid circular cylinder array [9, 10, 11]. In figure 3, a visualization is shown on how the velocity profiles for respectively rigid submerged and emergent vegetation should look like. Different from the emergent velocity profile, The horizontal velocity over the vertical scale of submerged vegetation shows obvious zonal characteristics. Using these zonal characteristics and momentum balance theory, various n-layers models have been developed to represent the full variation of the mean velocity distribution [10, 8]. The general approaches were summarized by Nepf [18]. To approximate the velocity profile for submerged vegetation with SWME is promising to do in combination with the multilayer approach.

In the next section, we will derive the shallow moment system with rigid emergent and submerged vegetation. Here the ideas will be used obtained from section 2 and include a new term for the friction caused by the vegetation.

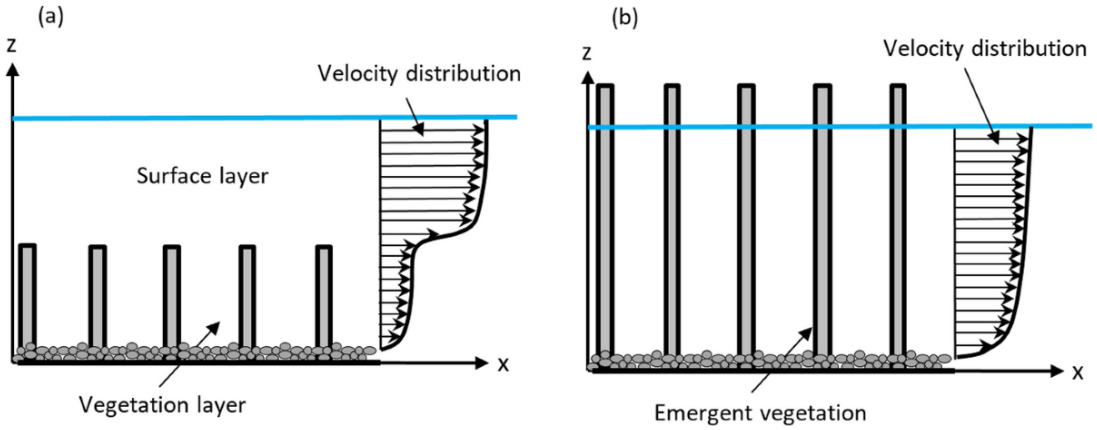

Figure 3: Visualization on how the velocity profiles should look like for rigid submerged (a) and emergent vegetation (b). Here you see how the velocity profile is affected by the vegetation

4 The SWME with vegetation

In this section, we will derive the SWME model with vegetation. First the focus will be on rigid emergent vegetation which is the simplest case. From here we will investigate the more complex case which is rigid submerged vegetation.

4.1 Emergent vegetation

As mentioned before, to incorporate the vegetation friction in our system, an extra term is implemented in the momentum balance equations from (1). The mass balance equation will

remain the same [5]. The modified Navier-Stokes equations are as follows:

$$\frac{\partial u}{\partial x}+\frac{\partial v}{\partial y}+\frac{\partial w}{\partial z}=0, \tag{25}$$

$$\frac{\partial u}{\partial t}+\frac{\partial u^2}{\partial x}+\frac{\partial uv}{\partial y}+\frac{\partial uw}{\partial z}=-F_x-\frac{1}{\rho}\frac{\partial p}{\partial x}+\frac{1}{\rho}\frac{\partial \sigma_{xz}}{\partial z}+ge_x, \tag{26}$$

$$\frac{\partial v}{\partial t}+\frac{\partial vu}{\partial x}+\frac{\partial v^2}{\partial y}+\frac{\partial vw}{\partial z}=-F_y-\frac{1}{\rho}\frac{\partial p}{\partial y}+\frac{1}{\rho}\frac{\partial \sigma_{yz}}{\partial z}+ge_y. \tag{27}$$

Here we have that the terms F_x and F_y are the vegetation friction per unit area in the respective x- and y-directions. The friction terms depend on the velocities u and v in the respective x- and y-directions, the drag coefficient C_d, the vegetation density per unit area N_v and the frontal frontal area of the vegetation A_v. The friction terms also depend on the z variable, since u and v vary over z and are not constant like in the SWE models. We us the following formulas for the vegetation friction [3]:

$$F_x=\frac{1}{2}C_dN_vA_vu\sqrt{u^2+v^2} \text{ and } F_y=\frac{1}{2}C_dN_vA_vv\sqrt{u^2+v^2}. \tag{28}$$

It is important to note that there are many other possibilities to define the vegetation friction.

Using this information we can derive the SWME with emergent vegetation in the same way as in section 2 by multiplying the momentum balance equations with h and use the transformations. We will only do this for the 1D case, since this is better to integrate. Then the friction term for the x-direction will reduce to:

$$F_x=\frac{1}{2}C_dN_vA_vu^2. \tag{29}$$

The x-momentum balance equation will then reduce to:

$$\frac{\partial}{\partial t}\left(h\hat{u}\right)+\frac{\partial}{\partial x}\left(h\hat{u}^2+\frac{g}{2}e_zh^2\right)+\frac{\partial}{\partial \zeta}\left(h\hat{u}\omega-\frac{1}{\rho}\hat{\sigma}_{xz}\right)=gh\left(e_x-e_z\frac{\partial h_b}{\partial x}\right)-h\hat{F}_x. \tag{30}$$

Where $\hat{F}_x$ denotes the vegetation friction F_x after the transformation

$$\hat{F}_x\left(x,\zeta,t\right)=\frac{1}{2}C_dN_vA_v\hat{u}\left(x,\zeta,t\right)^2. \tag{31}$$

Again for readability we drop the hat and integrate from 0 to 1 on both sides of equation (30) with respect to ζ. This results in the following:

$$\frac{\partial}{\partial t}\left(hu_m\right)+\frac{\partial}{\partial x}\left(h\left(u_m^2+\sum_{j=1}^{N}\frac{\alpha_j^2}{2j+1}\right)+\frac{g}{2}e_zh^2\right)=$$
$$-\frac{h}{2}C_dN_vA_v\int_0^1u^2d\zeta-\frac{\nu}{\lambda}\left(u_m+\sum_{j=1}^{N}\alpha_j\right)+gh\left(e_x-e_z\frac{\partial h_b}{\partial x}\right).$$

Using (17) the evolution equation for the mean velocity u_m with emergent vegetation is obtained:

$$\frac{\partial}{\partial t}\left(hu_m\right)+\frac{\partial}{\partial x}\left(h\left(u_m^2+\sum_{j=1}^{N}\frac{\alpha_j^2}{2j+1}\right)+\frac{g}{2}e_zh^2\right)=$$
$$-\frac{h}{2}C_dN_vA_v\left(u_m^2+\sum_{j=1}^{N}\frac{\alpha_j^2}{2j+1}\right)-\frac{\nu}{\lambda}\left(u_m+\sum_{j=1}^{N}\alpha_j\right)+gh\left(e_x-e_z\frac{\partial h_b}{\partial x}\right). \tag{32}$$

Next we need to find expressions for the coefficients α_i and β_i by again taking the moments of the velocity fields with respect to the shifted and scaled Legendre polynomials ϕ_j. We only have to focus on what happens to the vegetation drag term, since the rest of the equation is equal to (21). Hence the following integral is of interest

$$\begin{aligned}
\int_0^1 \phi_i F_x d\zeta &= \frac{1}{2} C_d N_v A_v \int_0^1 \phi_i u^2 d\zeta \\
&= \frac{1}{2} C_d N_v A_v \int_0^1 \left(\phi_i u_m^2 + 2u_m \sum_{j=1}^{N} \alpha_j \phi_j \phi_i + \phi_i \left(\sum_{j=1}^{N} \alpha_j \phi_j \right)^2 \right) d\zeta \\
&= \frac{1}{2} C_d N_v A_v \left(\frac{2u_m \alpha_i}{2i+1} + \sum_{j,k=1}^{N} \alpha_j \alpha_k \int_0^1 \phi_i \phi_j \phi_k d\zeta \right) \\
&= \frac{1}{2\,(2i+1)} C_d N_v A_v \left(2u_m \alpha_i + \sum_{j,k=1}^{N} \alpha_j \alpha_k A_{ijk} \right).
\end{aligned}$$

Where we used that the scaled Legendre polynomial of degree zero is one, $\phi_0 = 1$. Further, (23) is used in the last equality. Putting everything together we eventually obtain the resulting equation for α_i

$$\begin{aligned}
\frac{\partial}{\partial t}(h\alpha_i) + \frac{\partial}{\partial x}\left(h \left(2u_m \alpha_i + \sum_{j,k=1}^{N} \alpha_j \alpha_k A_{ijk} \right) \right) &= -\frac{h}{2} C_d N_v A_v \left(2u_m \alpha_i + \sum_{j,k=1}^{N} \alpha_j \alpha_k A_{ijk} \right) \\
+ u_m \frac{\partial}{\partial x}(h\alpha_i) - \sum_{j,k=1}^{N} \alpha_k B_{ijk} \frac{\partial}{\partial x}(h\alpha_i) - (2i+1)\frac{\nu}{\lambda} \left(u_m + \sum_{j=1}^{N} \left(1 + \frac{\lambda}{h} C_{ij} \right) \alpha_j \right). \quad (33)
\end{aligned}$$

The next section will investigate the case when the rigid circular cylinder vegetation is submerged and how we can derive the SWME system with this kind of vegetation.

4.2 Submerged vegetation

In the case where the rigid vegetation height is below the water surface height, $h_v < h$, we are dealing with submerged vegetation. Here h_v denotes the real vegetation height, $h_v = h_{vt} - h_b$ where h_{vt} denotes the top of the vegetation, in our reference system from the beginning of this paper (see figure 4). Here the vegetation height h_v can depend on the position x, since the height can be different at different other positions in the water. We will leave this for future work and set that the vegetation height is constant of over the position x. It is important to note that the vegetation drag force only affect the velocity in the region where the vegetation occurs, hence for rigid vegetation of length h_v, then when $h_b < z < h_{vt}$, F_x is equal to (29). In the region where $h_{vt} < z < h_s$, The vegetation friction will be zero, $F_x = 0$. Thus, the following formula for the vegetation friction is obtained

$$F_x(x,z,t) = \begin{cases} \frac{1}{2} C_d N_v A_v u(x,z,t), & \text{for } h_b < z < h_{vt}, \\ 0, & \text{for } h_{vt} < z < h_s. \end{cases} \quad (34)$$

We need to transform the rigid vegetation height h_v to the scaled space and do this by doing the following:

$$\delta_v = \frac{h_{vt} - h_b}{h} = \frac{h_v}{h}. \quad (35)$$

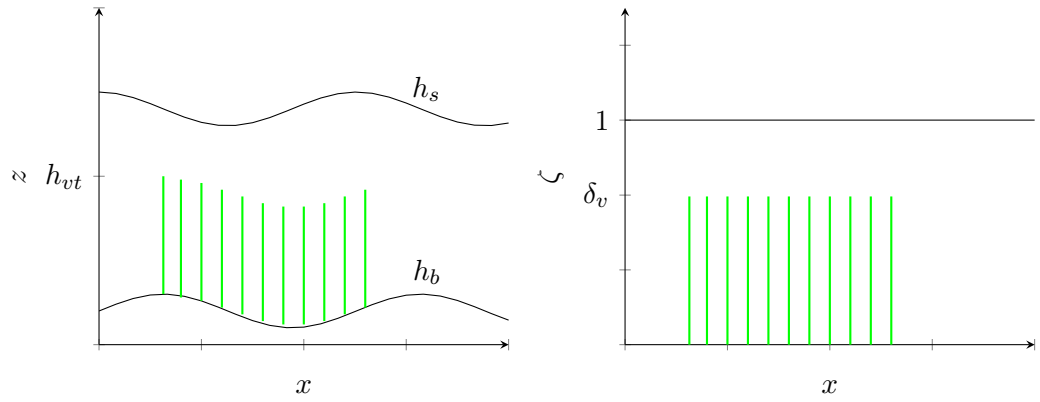

Figure 4: In the physical space (left), the vegetation height h_v is equal to the vegetation top h_{vt} minus the bottom topography h_b. Using the mapping (35) the vegetation height can be mapped to δ_v which is in the region $[0, 1]$.

Where δ_v is the dimensionless vegetation height in the scaled space and again use the transformation (5) which result in the following transformed vegetation friction formula

$$\hat{F}_x(x, \zeta, t) = \begin{cases} \frac{1}{2} C_d N_v A_v \hat{u}(x,\zeta,t), & \text{for } 0<\zeta<\delta_v, \\ 0, & \text{for } \delta_v<\zeta<1. \end{cases} \tag{36}$$

Hence, in the region $0 < \zeta < \delta_v$, the vegetation friction will affect the velocity and in the region $\delta_v < \zeta < 1$ it will be zero.

The starting point of the SWME system with submerged rigid vegetation is equation (30). Here we will integrate both sides from zero to one with respect to ζ. Then we have the following for the vegetation friction term:

$$\begin{aligned} \int_0^1 h F_x d\zeta &= h \int_0^{\delta_v} F_x d\zeta + h \int_{\delta_v}^1 F_x d\zeta \\ &= \frac{h}{2} C_d N_v A_v \int_0^{\delta_v} u^2 d\zeta \\ &= \frac{h}{2} C_d N_v A_v \int_0^{\delta_v} \left(u_m^2 + 2u_m \sum_{j=1}^N \alpha_j \phi_j + \left(\sum_{j=1}^N \alpha_j \phi_j \right)^2 \right) d\zeta. \end{aligned} \tag{37}$$

Here we use in the second equation the fact that $F_x = 0$ when $\delta_v < \zeta < 1$. The last integral can be dealt with term by term. The first term is straightforward, since u_m does not depend on ζ. The second term, on the other hand is already a bit more complicated, because we are now integrating over the interval $[0, \delta_v]$ and not over $[0, 1]$. Writing out this term results in:

$$\int_0^{\delta_v} 2u_m \sum_{j=1}^N \alpha_j \phi_j d\zeta = 2u_m \sum_{j=1}^N \alpha_j \int_0^{\delta_v} \phi_j d\zeta. \tag{38}$$

Before we can compute this integral we need the following property and definition of Legendre polynomials from [1].

Property 4.2.1 *Let $P_j(x)$ be the Legendre polynomial of degree j, then the following holds:*

$$P_j(x) = \frac{d}{d\zeta}\frac{P_{j+1}(x) - P_{j-1}(x)}{2j+1}. \tag{39}$$

$$P_j(-\zeta) = (-1)^j P_j(x). \tag{40}$$

$$P_j(1) = 1. \tag{41}$$

Definition 4.2.2 *Let $P_j(x)$ be the Legendre polynomial of degree j with $x \in [-1,1]$, then we have the following variable transformation $x(y) = 1 - 2y$ with $y \in [0,1]$. Since this variable transformation is bijective, it is also invertible. Hence, we can also define the transformation by $y(x) = \frac{1-x}{2}$. Then the shifted Legendre polynomials ϕ_j are defined as*

$$\phi_j(y) = P_j(x(y)). \tag{42}$$

Alternatively, one can define

$$\phi_j(y(x)) = P_j(x). \tag{43}$$

Using these properties, we can find a formula which looks like the formula of the Legendre polynomial (39) in the following way:

$$\begin{aligned}
P_j(x(y)) &= \frac{d}{dx(y)}\frac{P_{j+1}(x(y)) - P_{j-1}(x(y))}{2j+1} \\
\Rightarrow \phi_j(y) &= \frac{d}{dy}\frac{\phi_{j+1}(y) - \phi_{j-1}(y)}{2j+1}\frac{dy}{dx(y)} \\
\Rightarrow \phi_j(y) &= \frac{d}{dy}\frac{\phi_{j+1}(y) - \phi_{j-1}(y)}{2j+1}\frac{1}{\frac{dx(y)}{dy}} \\
\Rightarrow \phi_j(y) &= -\frac{d}{dy}\frac{\phi_{j+1}(y) - \phi_{j-1}(y)}{4j+2}.
\end{aligned}$$

and this is very useful in computing integrals of the shifted Legendre polynomial. Combining this with the fact that the shifted Legendre polynomial is normalized by $\phi_j(0) = 1$ for any j, we get

$$\begin{aligned}
\int_0^{\delta_v} \phi_j d\zeta &= \left[-\frac{\phi_{j+1}(\zeta) - \phi_{j-1}(\zeta)}{4j+2}\right]_0^{\delta_v} \\
&= -\frac{\phi_{j+1}(\delta_v) - \phi_{j-1}(\delta_v)}{4j+2} + \frac{\phi_{j+1}(0) - \phi_{j-1}(0)}{4j+2} \\
&= -\frac{\phi_{j+1}(\delta_v) - \phi_{j-1}(\delta_v)}{4j+2}.
\end{aligned}$$

This can be inserted back in (37) finishing the integral for this term. For the last term of (37), we first want to denote the following function depending on the rigid vegetation height:

$$Q_{jk}(\delta_v) = \int_0^{\delta_v} \phi_j \phi_k d\zeta. \tag{44}$$

We note here that Q_{jk} can be pre-computed if the vegetation height is known. Otherwise it can be computed at runtime analytically, but it does not need a approximation since it is just an integral of polynomials.

Using (44) the last term of (37) can be written in a different form resulting in

$$\begin{aligned}\int_0^{\delta_v}\left(\left(\sum_{j=1}^{N}\alpha_j\phi_j\right)^2\right)d\zeta &= \sum_{j,k=1}^{N}\alpha_j\alpha_k\int_0^{\delta_v}\phi_j\phi_k d\zeta \\ &= \sum_{j,k=1}^{N}\alpha_j\alpha_k Q_{jk}\left(\delta_v\right).\end{aligned}$$

Using (44) in the last equation. Combining everything we eventually obtain

$$\begin{aligned}\int_0^1 hF_x d\zeta &= \frac{h}{2}C_d N_v A_v\int_0^{\delta_v}\left(u_m^2+2u_m\sum_{j=1}^{N}\alpha_j\phi_j+\left(\sum_{j=1}^{N}\alpha_j\phi_j\right)^2\right)d\zeta \\ &= \frac{h}{2}C_d N_v A_v\left(u_m^2\delta_v-2u_m\sum_{j=1}^{N}\alpha_j\frac{\phi_{j+1}\left(\delta_v\right)-\phi_{j-1}\left(\delta_v\right)}{4j+2}+\sum_{j,k=1}^{N}\alpha_j\alpha_k Q_{jk}\left(\delta_v\right)\right).\end{aligned}$$

Inserting this back in the evolution equation for u_m, we finally get

$$\begin{aligned}\frac{\partial}{\partial t}\left(hu_m\right)+\frac{\partial}{\partial x}\left(h\left(u_m^2+\sum_{j=1}^{N}\frac{\alpha_j^2}{2j+1}\right)+\frac{g}{2}e_z h^2\right) = \\ -\frac{h}{2}C_d N_v A_v\left(u_m^2\delta_v-2u_m\sum_{j=1}^{N}\alpha_j\frac{\phi_{j+1}\left(\delta_v\right)-\phi_{j-1}\left(\delta_v\right)}{4j+2}+\sum_{j,k=1}^{N}\alpha_j\alpha_k Q_{jk}\left(\delta_v\right)\right) \\ -\frac{\nu}{\lambda}\left(u_m+\sum_{j=1}^{N}\alpha_j\right)+gh\left(e_x-e_z\frac{\partial h_b}{\partial x}\right). \quad (45)\end{aligned}$$

What may be interesting now, is to check whether (45) will go to (32) when the rigid submerged vegetation becomes emergent or, i.e. when $\delta_v \to 1$. Taking the first term after the equality of equation (45) and computing the limit

$$\begin{aligned}&\lim_{\delta_v\to 1}\frac{h}{2}C_d N_v A_v\left(u_m^2\delta_v-2u_m\sum_{j=1}^{N}\alpha_j\frac{\phi_{j+1}\left(\delta_v\right)-\phi_{j-1}\left(\delta_v\right)}{4j+2}+\sum_{j,k=1}^{N}\alpha_j\alpha_k Q_{jk}\left(\delta_v\right)\right) = \\ &\frac{h}{2}C_d N_v A_v\left(\lim_{\delta_v\to 1}u_m^2\delta_v-\lim_{\delta_v\to 1}2u_m\sum_{j=1}^{N}\alpha_j\frac{\phi_{j+1}\left(\delta_v\right)-\phi_{j-1}\left(\delta_v\right)}{4j+2}+\lim_{\delta_v\to 1}\sum_{j,k=1}^{N}\alpha_j\alpha_k Q_{jk}\left(\delta_v\right)\right). \quad (46)\end{aligned}$$

The first limit is straightforward. The second one is a bit more complicated and we need formu-

las (48) and (41) of property 4.2.1:

$$\begin{aligned}\phi_{j+1}(1)-\phi_{j-1}(1) &= P_{j+1}(-1)-P_{j-1}(-1)\\ &= (-1)^{j+1}P_{j+1}(1)-(-1)^{j-1}P_{j-1}(1)\\ &= (-1)^{j+1}-(-1)^{j-1}\\ &= -(-1)^{j}+(-1)^{j}\\ &= 0.\end{aligned}$$

Hence the second limit will go to zero. For the last limit it is important to remember that the shifted Legendre polynomial is orthogonal on the interval $[0,1]$ which means that

$$Q_{jk}(1)=\int_0^1 \phi_j\phi_k d\zeta=\frac{1}{2j+1}\delta_{jk}. \tag{47}$$

where $\delta_{jk}=1$ for $j=k$ and zero otherwise, hence

$$\begin{aligned}\lim_{\delta_v\to 1}\sum_{j,k=1}^{N}\alpha_j\alpha_k Q_{jk}(\delta_v) &= \sum_{j,k=1}^{N}\alpha_j\alpha_k Q_{jk}(1)\\ &= \sum_{j,k=1}^{N}\frac{\alpha_j\alpha_k}{2j+1}\delta_{jk}\\ &= \sum_{j,k=1}^{N}\frac{\alpha_j^2}{2j+1}.\end{aligned}$$

Putting this back in (46) we get

$$\frac{h}{2}C_dN_vA_v\left(\lim_{\delta_v\to 1}u_m^2\delta_v-\lim_{\delta_v\to 1}2u_m\sum_{j=1}^{N}\alpha_j\frac{\phi_{j+1}(\delta_v)-\phi_{j-1}(\delta_v)}{4j+2}+\lim_{h_v\to 1}\sum_{j,k=1}^{N}\alpha_j\alpha_k Q_{jk}(\delta_v)\right)=\frac{h}{2}C_dN_vA_v\left(u_m^2+\sum_{j,k=1}^{N}\frac{\alpha_j^2}{2j+1}\right).$$

Which is exactly the same as the vegetation friction term in the evolution equation of the mean velocity u_m (32) for the rigid emergent vegetation case of section 4.1.

Next, the expressions for the moment coefficients α_i are obtained by:

$$h\int_0^{\delta_v}\phi_i F_x d\zeta=\frac{h}{2}C_dN_vA_v\int_0^{\delta_v}\left(\phi_i u_m^2+2u_m\sum_{j=1}^{N}\alpha_j\phi_j\phi_i+\phi_i\left(\sum_{j=1}^{N}\alpha_j\phi_j\right)^2\right)d\zeta. \tag{48}$$

The integral over the first term is computed by using the recurrence formula which is also used for computing the second integral of the vegetation friction term of the evolution equation for the mean velocity u_m. The second integral results in:

$$2u_m\sum_{j=1}^{N}\alpha_j\int_0^{\delta_v}\phi_i\phi_j d\zeta=2u_m\sum_{j=1}^{N}\alpha_j Q_{ij}(\delta_v). \tag{49}$$

Where (44) is used, but now with respect to i and j. For the last integral, consider the following function:

$$A_{ijk}(\delta_v) = (2i+1)\int_0^{\delta_v} \phi_i\phi_j\phi_k d\zeta. \tag{50}$$

Here we remark the same as for Q_{jk} of (44). Now, we can compute the last integral as:

$$\begin{aligned}\int_0^{\delta_v} \phi_i \left(\sum_{j=1}^{N} \alpha_j\phi_j\right)^2 d\zeta &= \sum_{j,k=1}^{N} \alpha_j\alpha_k \int_0^{\delta_v} \phi_i\phi_j\phi_k d\zeta \\ &= \frac{1}{2i+1}\sum_{j,k=1}^{N} \alpha_j\alpha_k A_{ijk}\left(\delta_v\right)\end{aligned}$$

Combining everything and inserting it back in equation (48) we obtain:

$$\frac{h}{2}C_d N_v A_v \left(-u_m^2 \frac{\phi_{j+1}\left(\delta_v\right) - \phi_{j-1}\left(\delta_v\right)}{4j+2} + 2u_m \sum_{j=1}^{N} \alpha_j Q_{ij}(\delta_v) + \frac{1}{2i+1}\sum_{j,k=1}^{N} \alpha_j\alpha_k A_{ijk}(\delta_v)\right). \tag{51}$$

Hence, we obtain the following evolution equation for α_i:

$$\begin{aligned}&\frac{\partial}{\partial t}\left(h\alpha_i\right) + \frac{\partial}{\partial x}\left(h\left(2u_m\alpha_i + \sum_{j,k=1}^{N} \alpha_j\alpha_k A_{ijk}\right)\right) = \\ &-\frac{h}{2}C_d N_v A_v \left(-u_m^2 \frac{\phi_{j+1}\left(\delta_v\right) - \phi_{j-1}\left(\delta_v\right)}{4j+2} + 2u_m \sum_{j=1}^{N} \alpha_j Q_{ij}(\delta_v) + \frac{1}{2i+1}\sum_{j,k=1}^{N} \alpha_j\alpha_k A_{ijk}(\delta_v)\right) \\ &+ u_m D_i - \sum_{j,k=1}^{N} \alpha_k B_{ijk} D_i - (2i+1)\frac{\nu}{\lambda}\left(u_m + \sum_{j=1}^{N}\left(1 + \frac{\lambda}{h}C_{ij}\right)\alpha_j\right).\end{aligned} \tag{52}$$

When the rigid vegetation becomes emergent, $\delta_v \to 1$, we note that the first term of (51) will vanish, The second term can be computed by using (47) and for the third term $A_{ijk}(1) = A_{ijk}$. Hence, formula (52) will go to the evolution equation of α_i from the emergent vegetation case (33) of section 4.1.

In the next section, an analysis will be given to investigate how the dimensionless vegetation height δ_v will influence the vegetation friction term F_x for different velocity profiles.

5 Analysis of the vegetation friction term

In this section, an analysis will be given about the vegetation friction term. We will investigate how the vegetation friction term will grow for different velocity profiles with respect to the dimensionless vegetation height. In figure 5, the different velocity profiles, which will be investigated, are given. We want to make it clear that we only investigate the effect of the friction term on the momentum equation and not on the higher order coefficient equations.

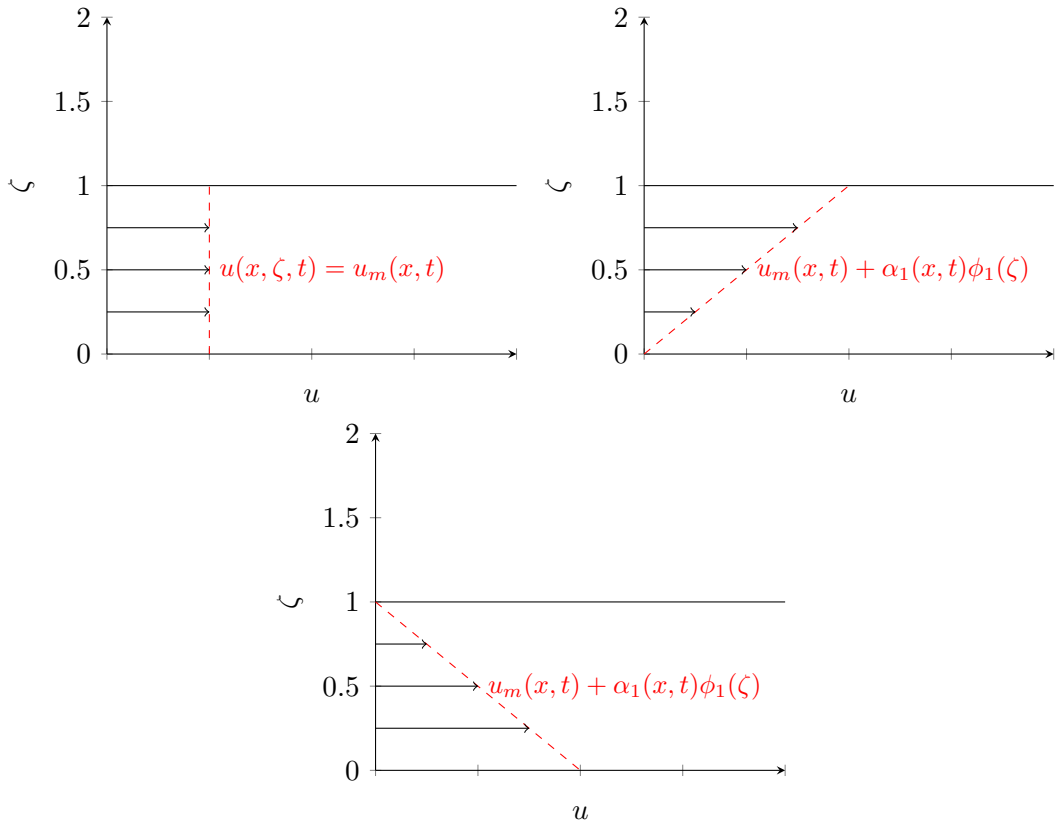

Figure 5: Velocity profiles for the case $N = 0$ (left above), $N = 1$ for $\alpha_1 = -u_m$ (right above) and $N = 1$ for $\alpha_1 = u_m$ (below).

First we remember the moment expansion of the velocity (15) and use the assumption that we have a linear velocity profile ($N = 1$), then the moment expansion will reduce to:

$$\begin{aligned} u(x,\zeta,t) &= u_m(x,t) + \sum_{j=1}^{1} \alpha_j(x,t)\,\phi_j(\zeta) \\ &= u_m(x,t) + \alpha_1(x,t)\,\phi_1(\zeta)\,. \end{aligned}$$

As seen in figure 5. Important to note is that $\alpha_1 \in [-u_m, u_m]$. When α_1 is equal to $-u_m$ or u_m, then the respective velocity profiles looks like the second and the third figure. The velocity profiles will get steeper when α_1 goes to zero and if $\alpha_1 = 0$ the average case is obtained (first figure). We exclude the case where $\alpha_1 > u_m$ or $\alpha_1 < -u_m$, since this leads to a change in sign for the velocity, which might lead to small scale phenomena in the flow that are not considered in the shallow flow assumption (see figure 6).

Going back to the friction term of the evolution equation of the mean velocity u_m (45), then for the average case when $N = 0$ the vegetation friction term will go to:

$$\frac{h}{2} C_d N_v A_v \left(u_m^2 \delta_v - 2u_m \sum_{j=1}^{N} \alpha_j \frac{\phi_{j+1}(\delta_v) - \phi_{j-1}(\delta_v)}{4j+2} + \sum_{j,k=1}^{N} \alpha_j \alpha_k Q_{jk}(\delta_v) \right) = \frac{h}{2} C_d N_v A_v u_m^2 \delta_v. \tag{53}$$

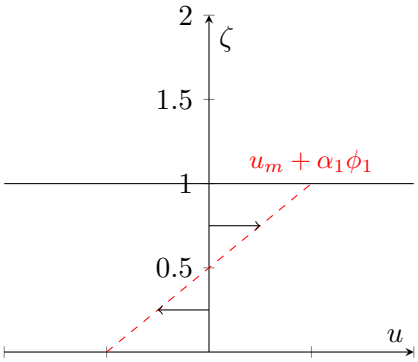

Figure 6: Velocity profile when $\alpha_1 < -u_m$.

Looking at this equation, it can been seen that we can take out the square resulting in the following:

$$\frac{h}{2}C_d N_v A_v u_m^2 \delta_v = \frac{h}{2}C_d N_v A_v u_m \sqrt{\delta_v} u_m \sqrt{\delta_v}.$$

Using (35) we obtain:

$$\begin{aligned}\frac{h}{2}C_d N_v A_v u_m \sqrt{\delta_v} u_m \sqrt{\delta_v} &= \frac{h}{2}C_d N_v A_v u_m \sqrt{\frac{h_v}{h}} u_m \sqrt{\frac{h_v}{h}} \\ &= \frac{h}{2}C_d N_v A_v u_v^2\end{aligned}$$

Where $u_v = u_m\sqrt{\frac{h_v}{h}}$ denotes the apparent velocity which was proposed by Stone and Shen [19]. When the rigid vegetation is emergent, the apparent velocity will be $u_v = u$.

The more interesting case is when the velocity profile is linear, then for the vegetation friction term we can fill in $N = 1$, which results in:

$$\begin{aligned}&\frac{h}{2}C_d N_v A_v \left(u_m^2\delta_v - 2u_m\alpha_1\frac{\phi_2(\delta_v) - \phi_0(\delta_v)}{6} + \alpha_1^2 Q_{11}(\delta_v)\right), \\ \Rightarrow &\frac{h}{2}C_d N_v A_v \left(u_m^2\delta_v - 2u_m\alpha_1\frac{1 - 6\delta_v + 6\delta_v^2 - 1}{6} + \alpha_1^2\int_0^{\delta_v}\phi_1^2 d\zeta\right), \\ \Rightarrow &\frac{h}{2}C_d N_v A_v \left(u_m^2\delta_v - 2u_m\alpha_1\left(\delta_v^2 - \delta_v\right) + \alpha_1^2\int_0^{\delta_v}(1-2\zeta)^2 d\zeta\right), \\ \Rightarrow &\frac{h}{2}C_d N_v A_v \left(u_m^2\delta_v - 2u_m\alpha_1\left(\delta_v^2 - \delta_v\right) + \alpha_1^2\left(\delta_v - 2\delta_v^2 + \frac{4}{3}\delta_v^3\right)\right).\end{aligned}$$

Using this formula, we can plot the vegetation friction term and see how this will increase when the dimensionless vegetation height δ_v varies between zero and 1 for different values of $\alpha_1 \in [-u_m, u_m]$. First we note that for linear increasing velocity profile like in the second figure of 5, we see that for short vegetation height the vegetation friction term should have small friction for short vegetation. When the vegetation height grows, the vegetation friction term should grow increasingly fast. If the velocity profile is linear decreasing like in the third figure of 5, we have the opposite. For short vegetation, the vegetation friction should be high and when

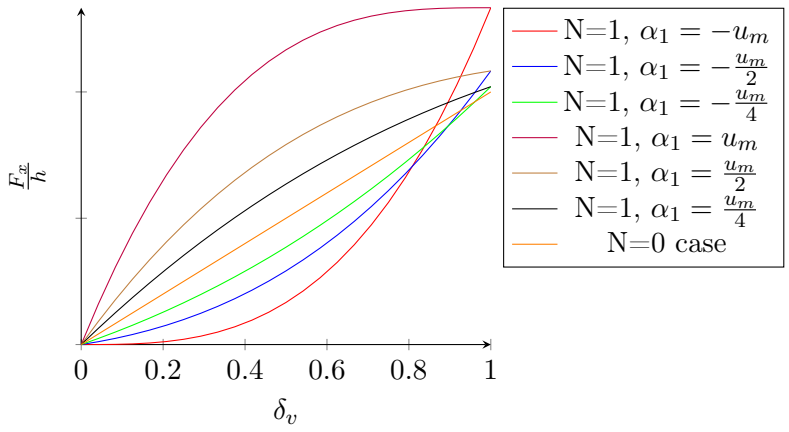

Figure 7: The vegetation friction increase over the dimensionless vegetation height δ_v, for the constant and linear velocity profiles with respective order $N = 0$ and $N = 1$, for different values $\alpha_1 \in [-u_m, u_m]$.

the vegetation height grows higher, the friction increase should flatten out. Eventually, for both cases the vegetation friction term should be equal when the vegetation is emergent, since both cases have the same velocity profile only they are the opposites of each other.

In figure 7, the different vegetation friction increase trajectories are displayed over the the dimensionless vegetation height δ_v. Where the drag coefficient C_d, vegetation density per unit area N_v and the frontal area of the vegetation A_v stays constant. When these constants are changed, we obtain the same results. Further we will divide F_x with the water depth such that the friction will be dimensionless. The first interesting point obtained from 7 is that for the constant velocity case $N = 0$, we have a linear friction increase over the vegetation height. From the first figure of 5 this makes sense, since the horizontal velocity stays the same over the vertical scale. The following point which can be obtained is when the velocity has a linear increasing profile $N = 1$ and $\alpha_1 = -u_m$, then as expected, there is small friction for short vegetation height. When δ_v grows larger, we observe a rapid increase of the vegetation friction. When the increasing linear velocity profile becomes steeper, for example for $\alpha_1 = -\frac{u_m}{2}$ and $\alpha_1 = -\frac{u_m}{4}$, there is higher velocity at the bottom, than for $\alpha_1 = -u_m$. Hence, there is more friction for short vegetation, but will increase less faster later. Eventually, for emergent vegetation $\delta_v = 1$, the friction for the case $\alpha_1 = -u_m$ is higher than for the steeper linear increase velocity profiles. This happens due to the fact that the velocity in the vegetation friction formula (29) is squared. Hence, because the velocity is higher at the water surface for $\alpha_1 = -u_m$ than for the steeper cases, thus the friction is also higher when the vegetation is emergent. Next, when the velocity has a decreasing linear profile, $\alpha_1 = u_m$ the friction will be high for short vegetation and will flatten out over the vegetation height. When the decreasing velocity profile becomes steeper, the velocity at the bottom will be slower, which leads to less friction for short vegetation. Furthermore, the friction for decreasing velocity profile equals with there respective increasing velocity profiles when the vegetation is emergent. Other points which can be observed from figure 7 is that when α_1 goes to zero, the friction increase converges to a linear line equal to the constant velocity profile. For emerging vegetation, the linear velocity profile always increases the friction and for submerged vegetation it depends on α_1 whether the friction is larger or smaller than that for the constant case.

It is important to note that there are some limitations on the research done in this paper, but can be investigated in future work. Here we only investigated friction increase when velocity profile is constant ($N = 0$) or linear ($N = 1$), but not for higher orders which should be investigated too. Further, we showed the friction increase over the vegetation height, but it is also interesting to see what happens when the mean velocity changes for different vegetation heights. Other limitations are the vegetation friction effect on the higher order equations or what happens to the SWME when the vegetation is floating. All these limitations can be taking into account in future work on this topic.

6 Conclusion

In this paper we derived the shallow water moment system for rigid submerged and emergent vegetation by introducing a new term for the vegetation friction. Here the vegetation was represented by a circular cylinder with uniform diameter. The vegetation friction term from the evolution equation of the mean velocity gave a logical increase over the vegetation height.

After a brief introduction about the importance of the topic the derivation of the SWME was reviewed and explained the importance of the transformation and expansion ideas. Further, a brief introduction has been given on some research done on how vegetation can affect the velocity profiles in rivers.

Using the information gained, a vegetation friction term was included into the reduced incompressible Navier-Stokes equations. With the help of the transformation and expansion idea the shallow moment system was derived with rigid emergent and submerged vegetation. Where for submerged vegetation there is only friction in the region where vegetation is present. Hence, when we integrate to derive the evolution equations for the shallow moment system, over the water depth. We only need to integrate the friction formula over the vegetation height.

In the analysis we showed using the derived evolution equation of the mean velocity the vegetation friction increase over the vegetation height for a constant, linear increasing, and linear decreasing velocity profiles for various different values of the moment coefficient. Here we obtained that for a linear increasing velocity profile there is small friction for short vegetation, but will increase rapidly later just as expected. For the decreasing case there is a direct opposite behaviour.

It is important to note that the research done in this paper is a beginning in describing the water flow with vegetation, since we only show the friction increases when the velocity profiles are constant or linear. It can be interesting to investigate the friction increase over the vegetation height when the order $N > 1$ or what happens when the vegetation is floating. Other research can be done by simulating the derived SWME with vegetation for real life scenarios. Furthermore, in this paper we simplified the representation of the vegetation into a rigid circular cylinder, where in reality vegetation can have a more complex geometry which can interact with the flow differently. Hence, there is still a lot of research which can be done by future work.

References

[1] G. B. Arfken and H. J. Weber. “Mathematical methods for physicists”. In: Elsevier Academic Press, 2005. Chap. 12.2.

[2] S. Arora and B. Kumar. “Effect of emergent vegetation on riverbank erosion with sediment mining”. In: *Scientific Reports* 14.11193 (2024), pp. 1–17.

[3] F. Bai, Z. Yang, W. Huai, and C. Zheng. "A depth-averaged two dimensional shallow water model to simulate flow-rigid vegetation interactions". In: *Procedia Engineering* 154 (2016), pp. 482–489.

[4] Z. Cai, Y. Fan, and R. Li. "On hyperbolicity of 13-moment system". In: *Kinetic and Related Models* 7.3 (2014), pp. 415–432.

[5] K. S. Erduran. "Quasi-three-dimensional numerical model for flow through flexible rigid submerged and non-submerged vegetation". In: *Journal of Hydroinformatics* 5.3 (2003), pp. 189–202.

[6] Y. Fan, J. Koellermeier, J. Li, R. Li, and M. Torrilhon. "Model reduction of kinetic equations by operator projection". In: *Journal of Statistical Physics* 162.2 (2016), pp. 1021–1065.

[7] R. van Hespen, Z. Hu, B. Borsje, M. De Dominicis, D. A. Friess, S. Jevrejeva, M. G. Kleinhans, M. Maza, C. E.J. van Bijsterveldt, T. Van der Stocken, B. van Wesenbeeck, D. Xie, and T. J. Bouma. "Mangrove forests as a nature-based solution for coastal flood protection: Biophysical and ecological considerations". In: *Water Science and Engineering* 16.1 (2023), pp. 1–13.

[8] W. Huai, Z. Chen, and J. Han. "Mathematical model for the flow with submerged and emerged rigid vegetation". In: *Journal of Hydrodynamics* 21.5 (2009), pp. 722–729.

[9] W. Huai, S. Li, G. G. Katul, M. Liu, and Z. Yang. "Flow dynamics and sediment transport in vegetated rivers: A review". In: *Journal of Hydrodynamics* 33.3 (2021), pp. 400–420.

[10] W. Huai, Y. Zeng, W. Wang, and Z. Yang. "Analytical model of the mean velocity distribution in an open channel with double-layered rigid vegetation". In: *Advances in Water Resources* 69 (2014), pp. 106–113.

[11] W. Huai, Y. Zeng, W. Wang, and Z. Yang. "Numerical Investigation of Focused Waves and Their Interaction With a Vertical Cylinder Using REEF3D". In: *Journal of Offshore Mechanics and Arctic Engineering* 139.4 (2017).

[12] H. Kanayama and H. Dan. "A tsunami simulation of Hakata Bay using the viscous shallow-water equation". In: *Japan Journal of Industrial and Applied Mathematic* 30.3 (2013), pp. 605–624.

[13] J. Koellermeier and M. Rominger. "Analysis and Numerical Simulation of Hyperbolic Shallow Water Moment Equations". In: (2020).

[14] J. Kowalski and M. Torrilhon. "Moment Approximations and Model Cascades for Shallow Flow". In: *Communications in Computational Physics* 25.3 (2019), pp. 669–702.

[15] R. J. LeVeque. *Finite Volume Methods for Hyperbolic Problems*. Cambridge Texts in Applied Mathematics. Cambridge University Press, 2002.

[16] D. Levermore. "Moment closure hierarchies for kinetic theories". In: *Journal of Statistical Physics* 83.5 (1996), pp. 1021–1065.

[17] I. Nagelkerken, S.J.M. Blaber, S. Bouillon, P. Green, M. Haywood, L.G. Kirton, J.-O. Meynecke, J. Pawlik, H.M. Penrose, A. Sasekumar, and P.J. Somerfield. "The habitat function of mangroves for terrestrial and marine fauna: A review". In: *Aquatic Botany* 89.2 (2008), pp. 155–185.

[18] H. M. Nepf. "Flow and transport in regions with aquatic vegetation". In: *Annual Review of Fluid Mechanics* 44 (2012), pp. 123–142.

[19] B. M. Stone and H.T. Shen. "Hydraulic resistance of flow in channels with cylindrical roughness". In: *Journal of Hydraulic Engineering* 128.5 (2002), pp. 500–506.

[20] M. Taphorn, R. Villanueva, M. Paul, J. Visscher, and T. Schlurmann. "Flow field and wake structure characteristics imposed by single seagrass blade surrogates". In: *Journaal of ecohydraulics* 7.1 (2022), pp. 58–70.

[21] T. Tiggeloven, H. de Moel, V. van Zelst, B. van Wesenbeeck, H. Winsemius, D. Eilander, and P. Ward. "The benefits of coastal adaptation through conservation of foreshore vegetation". In: (2022).

[22] H. Weller and H. G. Weller. "A high-order arbitrarily unstructured finite-volume model of the global atmosphere: Tests solving the shallow-water equations". In: *International Journal for Numerical Methods in Fluids* 56.8 (2008), pp. 1589–1596.